J. Fluid Mech. (1970), *vol.* 42, *part* 3, *pp.* 609–625
Printed in Great Britain

The flow of a tubular film Part 2. Interpretation of the model and discussion of solutions

By J. R. A. PEARSON AND C. J. S. PETRIE†
Department of Chemical Engineering, University of Cambridge

(Received 3 September 1969)

The equations governing the free-surface flow of a tubular film of liquid are derived from physical arguments, which throw some light on the formal process described in part 1. The solutions of the equations are discussed, in particular with reference to the film-blowing process for the manufacture of thin sheets of thermoplastic material. The qualitative adequacy of a model based on the dominance of viscous forces is demonstrated, and the effect of surface tension, air drag and non-isothermal flow is discussed briefly.

1. Introduction

The work described below can be thought of either as an application of the formal results of part 1 (Pearson & Petrie 1970*a*), providing in addition a physical description of the approximations made there, or as a physically based approximate solution of a practical problem, whose formal justification can be found in part 1. The authors hope that they have succeeded in separating the two parts of the work sufficiently for either to be intelligible on its own.

The process studied here is one for the manufacture of a thin sheet or film of a thermoplastic, such as polyethylene, from molten material supplied under pressure by a screw extruder. Figure 1 illustrates the process schematically. The liquid is forced through an annular die and the tubular film produced is thinned by both an internal pressure and an axial tension. Thus, any element of the film is being drawn down in two directions as it flows from the die to the take-up rolls (which are usually vertically above the die). These are arranged to guide the film once it has solidified (and cooled sufficiently to prevent the film sticking to itself) from its cylindrical shape to a plane ('layflat') form as it passes through the nip rolls. The nip rolls form an airtight seal, so that between them and the die the film forms a tubular bubble containg air at a pressure slightly above atmospheric. The air supply led in through the centre of the die is used only to adjust this pressure.

The rate of cooling, and thus the distance to the freeze-line (the region where the molten polymer solidifies) is controlled by jets of cooling air from a ring sur-

† Present address: Department of Engineering Mathematics, University of Newcastle upon Tyne.

rounding the bubble. The nip rolls are driven to provide the axial tension needed to take up the film, and might be driven at either constant speed or constant torque, usually the former. (The implications of this choice for the problem of the control of product dimensions are discussed elsewhere—Pearson & Petrie 1970*b*.)

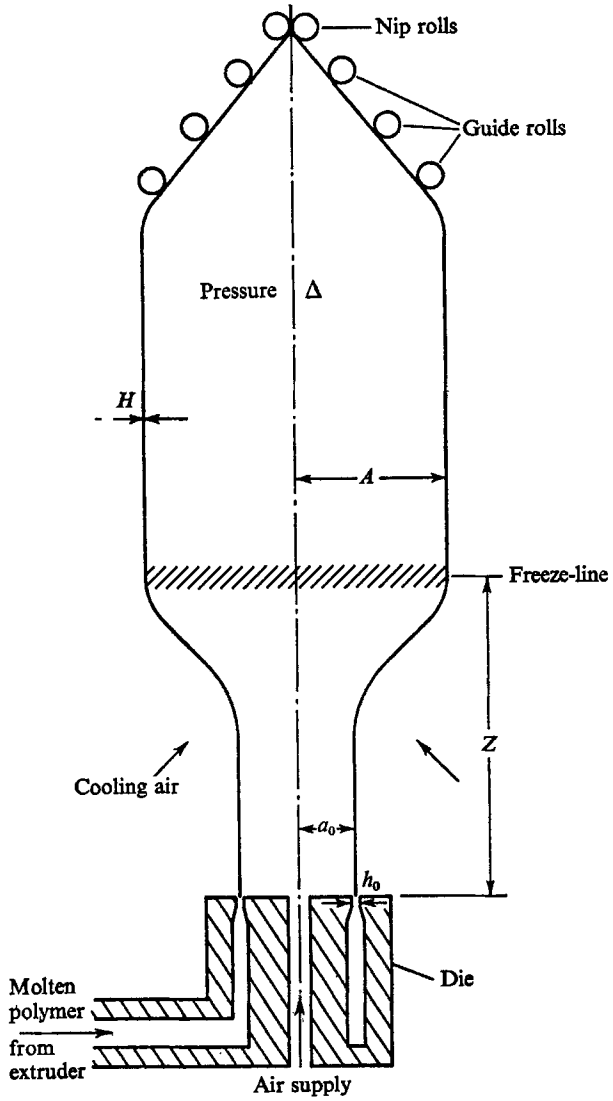

FIGURE 1. Diagram of the film-blowing process; section in a vertical plane.

As far as the steady-state problem is concerned we can take either the speed or the torque as prescribed, and the choice which is most convenient for our analysis of the flow of the liquid polymer is of a given axial tension applied to the film at the freeze-line.

What we seek to do here is to set up and use a mathematical model of the flow in the region between the die and the freeze-line, where we have the free-surface

flow of a highly viscous liquid. We need to prescribe at least seven parameters in order to get a determinate problem, and these are taken to be the bubble radius and the film thickness at the die, the freeze-line distance, the pressure difference across the bubble, the axial tension at the freeze-line, the volumetric flow rate, and the viscosity of the liquid. If we wish to take account of any but the essential factors controlling the flow, more parameters will be required. We can then predict the bubble shape, its thickness and velocity, and the forces acting in it. In particular, the dimensionless ratios of bubble radius, film thickness and velocity at the freeze-line to the corresponding quantities at the die can be predicted in terms of three numbers, which are essentially dimensionless values of the freeze-line distance, the excess pressure inside the bubble, and the axial tension at the freeze-line. (The velocity ratio and the axial tension can be transposed between the lists of dependent and independent quantities, if the velocity, rather than the tension, is prescribed at the freeze-line.)

2. The mathematical model

The basic assumptions made are that the forces controlling the flow are the viscous forces arising in the steady axisymmetric isothermal flow of a homogeneous Newtonian liquid, and that the film is thin enough for variations in the flow field across it to be ignored, and for the velocity gradients to be approximated locally by those of a plane film being extended bi-axially. These assumptions, and the neglect of the effects of gravity, surface tension, air drag and the inertia of the liquid, are justified formally to some extent in part 1. They are justified practically, in part at least, by the fact that reasonable predictions are obtained.

Further experimental verification is required before the range of applicability of the simple viscous model can be inferred. Certainly cases are known where other factors cannot be neglected, in particular gravity. The present model can be extended to cover most of these cases.

Equations governing the flow have already been derived in part 1 (equations (16) and (17)) by means of a formal perturbation expansion. Here an alternative, less formal, approach is shown to lead to the same results, and at the same time to help in the understanding of the essential physics of the situation. The two relevant equations are based on a simple balance of forces, one in the axial direction and the other in the direction normal to the film surface.

We take cylindrical polar co-ordinates (ρ, ϕ, z) as shown in figures 1 and 2, and define the following symbols:

a is the bubble radius (measured normal to the z-axis) which takes values a_0 at $z = 0$ (at the die) and A at $z = Z$ (at the freeze-line); corresponding dimensionless quantities are $r = a/a_0$ and $R = A/a_0$. (r corresponds to h_{03} in part 1.)

h is the film thickness (measured normal to the film surface), which takes the values h_0 at $z = 0$ and H at $z = Z$; since h only appears as a ratio, it is not necessary to define a dimensionless thickness. (h/a_0 corresponds to ϵh_{12} in part 1.)

$x = z/a_0$ and $X = Z/a_0$ are dimensionless values of the axial co-ordinate and of the freeze-line distance respectively.

θ is the angle between the bubble profile and the z-axis, so that $\tan\theta = da/dz$.

μ is the liquid viscosity and Q the total volumetric flow rate.

Δ is the pressure difference across the bubble, p (inside) $-p$ (outside), and F_Z is the axial force applied at the freeze-line.

In order to obtain the velocity gradients, we define local Cartesian co-ordinates (ξ_1, ξ_2, ξ_3) at a point P in the film, with ξ_1 in the direction of flow, ξ_2 normal to the film and ξ_3 in the transverse (circumferential) direction (see figure 2). For definiteness we take the origin P to be on the inner surface; then the ξ_2-axis

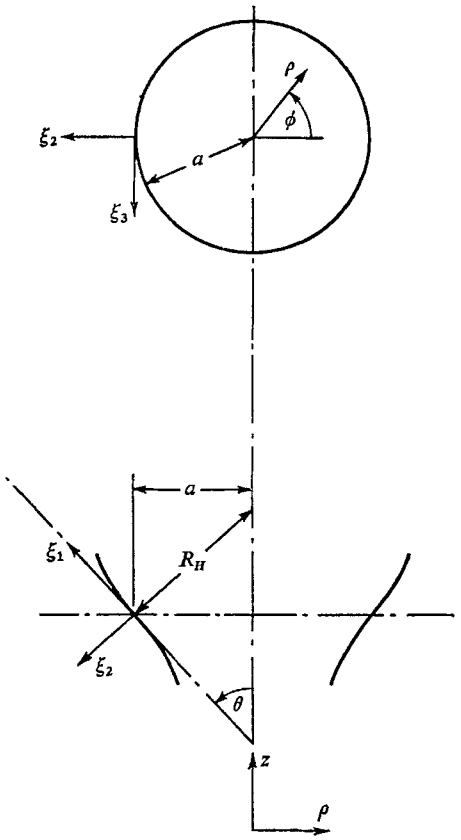

FIGURE 2. Co-ordinate systems; sectioned plan and elevation of a portion of the film.

meets the outer surface at $\xi_2 = h$. (At P, the ξ_i directions coincide with the x_i directions of the 'intrinsic' co-ordinates used in part 1.) In this co-ordinate system, we take velocity components (v_1, v_2, v_3), and proceed to obtain approximations to the velocity gradients $\partial v_i/\partial \xi_j$.

On the inner surface $\xi_2 = 0$, v_2 is zero, and on the outer surface $v_2 = Dh/Dt$, so that, neglecting the variation of $\partial v_2/\partial \xi_2$ with ξ_2, we obtain

$$\partial v_2/\partial \xi_2 = h^{-1} Dh/Dt.$$

Similarly, using the axisymmetry condition and the relation $\xi_3 = a \tan \phi$, we obtain

$$\partial v_3/\partial \xi_3 = a^{-1} Da/Dt;$$

and continuity gives

$$\partial v_1/\partial \xi_1 = -(h^{-1}Dh/Dt + a^{-1}Da/Dt).$$

These quantities are all $O(1)$; the other velocity gradients are $O(h/a)$; they are ignored in this analysis. Treating a and h as functions of z, and using $dz/d\xi_1 = \cos\theta$ and $D\xi_1/Dt = v_1$, we obtain

$$\partial v_1/\partial \xi_1 = -v_1 \cos\theta (a^{-1}da/dz + h^{-1}dh/dz).$$

$$\partial v_2/\partial \xi_2 = v_1 \cos\theta\, h^{-1}dh/dz,$$

and

$$\partial v_3/\partial \xi_3 = v_1 \cos\theta\, a^{-1}da/dz.$$

(It may readily be shown that these correspond to the first-order terms obtainable from equation (3), part 1.)

The principal stresses are given by

$$p_{ii} = -p + 2\mu\, \partial v_i/\partial \xi_i, \quad \text{for} \quad i = 1, 2, \text{ and } 3,$$

and the condition that p_{22} is zero (relative to atmospheric pressure) at the free surfaces gives, for the hydrostatic pressure p,

$$p = 2\mu v_1 \cos\theta\, h^{-1}dh/dz \tag{1}$$

(cf. equation (15), part 1). This imposes the condition that $\Delta \ll p$; i.e. Δ is $O(h/a)$ multiplied by a typical viscous stress. (There is no inconsistency in ignoring Δ here while using it below, since in the equations below it balances terms of order h multiplied by a typical viscous stress.) The stresses are functions of ξ_1 only; and they can be integrated across the film to give the longitudinal and transverse (hoop) forces per unit length, P_L ($= hp_{11}$) and P_H ($= hp_{33}$), respectively. Using the overall equation of continuity, $Q = 2\pi a h v_1$, to eliminate v_1 gives finally

$$P_L = -\frac{\mu Q \cos\theta}{\pi a}\left\{\frac{1}{a}\frac{da}{dz} + \frac{2}{h}\frac{dh}{dz}\right\}, \tag{2}$$

and

$$P_H = \frac{\mu Q \cos\theta}{\pi a}\left\{\frac{1}{a}\frac{da}{dz} - \frac{1}{h}\frac{dh}{dz}\right\}. \tag{3}$$

The balance of the total axial force between cross-sections at z and at Z (the freeze-line) gives, neglecting inertial forces,

$$2\pi a P_L \cos\theta - \pi a^2 \Delta = F_Z - \pi A^2 \Delta; \tag{4}$$

that of the normal forces on the film gives

$$\Delta = P_L/R_L + P_H/R_H, \tag{5}$$

where R_L and R_H are the principal radii of curvature,

$$R_H = a\sec\theta \quad \text{and} \quad R_L = -\sec^3\theta/(d^2a/dz^2).$$

(See e.g. Novozhilov 1959, p. 96.)

Introducing the dimensionless variables defined above and the dimensionless parameters,

$B = \pi a_0^3 \Delta/\mu Q$ (a dimensionless pressure difference),

$T_Z = a_0 F_Z/\mu Q$ (a dimensionless axial force),

and $T = T_Z - R^2 B$ (the total dimensionless axial force at any cross-section),

and writing $'$ for d/dx give, after some rearrangement,

$$h'/h = -\tfrac{1}{2}r'/r - \tfrac{1}{4}\sec^2\theta(T + r^2 B) = -\tfrac{1}{2}r'/r - \tfrac{1}{4}(1+r'^2)(T + r^2 B), \tag{6}$$

and

$$2r^2(T + r^2 B)\, r'' = 6r' + r\sec^2\theta(T - 3r^2 B) = 6r' + r(1+r'^2)(T - 3r^2 B). \tag{7}$$

(In order to show the equivalence of these equations to (16) and (17), part 1, set $B = P_1/2\phi_0$, $dx/dx^1 = \cos\theta$, and eliminate T by differentiation.) Thus, we have found one integral of the equations derived in part 1, and have separated the problem of finding the shape of the bubble from that of finding the film thickness, (7) being an equation in r alone.

Two boundary conditions for (6) and (7) can be stated immediately. They are

$$h = h_0, \quad r = 1 \quad \text{at} \quad x = 0. \tag{8}$$

A second boundary condition for (7) could be prescribed arbitrarily as

$$r' = b \quad \text{at} \quad x = 0,$$

but physical considerations suggest that it is conditions at the freeze-line end of the bubble that will control the process. If the material freezes (i.e. $\mu \to \infty$), then r' must become zero beyond that line, no further deformation being possible. It is intuitively obvious that the relation,

$$r' = 0, \quad x = X, \tag{9}$$

can be applied to the molten region also, provided P_L and P_H remain bounded. To show this in the case of rapid freezing, we suppose that the viscosity changes from its constant finite value μ_0 to an infinite value within a region of length e (measured in the x-direction) where ϵ can later $\to 0$. If this is the case, then r can be taken as constant in (7) and we get a relation of the form,

$$r'' = A\mu r' + B(1+r'^2).$$

Here A and B are constants, fixed by the parameters defining the problem, $r' = 0$ at $x = X$ and μ varies from μ_0 to infinity in the range $[X-\epsilon, X]$. Elementary argument shows that for suitable μ, say

$$\mu = \mu_0(\epsilon/(X-x))^{\frac{1}{2}},$$

the term r'' is always $O(1)$ and so r' is always $O(\epsilon)$. Hence, by letting $\epsilon \to 0$, we recover (9) as the suitable boundary condition we sought. It is worth noting that the same argument does not imply $h' = 0$ at $x = X$, which would otherwise overdetermine the problem.

The consequence of these boundary conditions is that the solution of (6), (7) will not in general yield $r' = 0$ at $x = 0$, although for large enough X this is very

nearly true. This is not incompatible with the equations governing flow at a die exit; though at the level of approximation we are concerned with, we cannot investigate this matter further.

3. Discussion

3.1. *The phase-plane*

We now have a non-linear two-point boundary-value problem; both for the qualitative discussion, and for the numerical solution of (7), it is convenient to take initial conditions $r = R$, $r' = 0$ at $x = X$, then modify the choice of R until we get $r = 1$ at $x = 0$. From this point of view, the parameters B (pressure), T_Z (axial tension), X (freeze-line distance) and the initial value R completely specify the bubble shape ($T = T_Z - R^2B$), and we avoid the problem that, if we start from $x = 0$, R and hence the parameter T, which appears in the equation, are not known in advance. (It would be necessary to guess values for r' at $x = 0$ and for T, two guesses instead of one.)

We rewrite (7) as

$$\left.\begin{aligned} dr/dx &= s, \\ ds/dx &= \{6s + r(1+s^2)\,(T - 3r^2B)\}/\{2r^2(T + r^2B)\}, \end{aligned}\right\} \tag{10}$$

and study the trajectories (solution curves) of system (10) in the phase plane with co-ordinates (r, s). The system

$$\left.\begin{aligned} dr/d\xi &= -2r^2s(T + r^2B), \\ ds/d\xi &= -6s - r(1+s^2)\,(T - 3r^2B), \end{aligned}\right\} \tag{11}$$

where $dx/d\xi = -2r^2(T + r^2B)$, has the same trajectories as system (10), with x decreasing in the direction of ξ increasing for $r^2(T + r^2B) > 0$. Problems of interpretation on $r = 0$ and on $T + r^2B = 0$ will be postponed.

Since the equations are unaltered if the signs of r and s are both changed, and since the half-lines $r = 0, s > 0$ and $r = 0, s < 0$ are solutions of system (11), and so may not be crossed by any other trajectories, we confine our attention to the half-plane $r \geqslant 0$. In order to keep the discussion manageable, we restrict attention to $B > 0$ and $T_Z > 0$, the ranges relevant to the problem which motivates this study, and consider the three cases $T > 0$, $T = 0$ and $T < 0$. These are further subdivided, according to the number and type of the singular points, into:

$$\begin{aligned} &1(a), \quad T^3 > 81B/16 > 0, \\ &1(b), \quad T^3 = 81B/16 > 0, \\ &1(c), \quad 81B/16 > T^3 > 0, \\ &2, \quad T = 0, \\ &3(a), \quad 0 > T^3 > -9B/16, \\ &3(b), \quad 0 > T^3 = -9B/16, \\ &3(c), \quad 0 > -9B/16 > T^3. \end{aligned}$$

The results are summarized here and illustrated in figures 3–5. The appendix gives more details and outlines proofs of some of the statements made here.

Case 1. There are two singular points in $r \geqslant 0$, namely $(0, 0)$, which is a saddle-

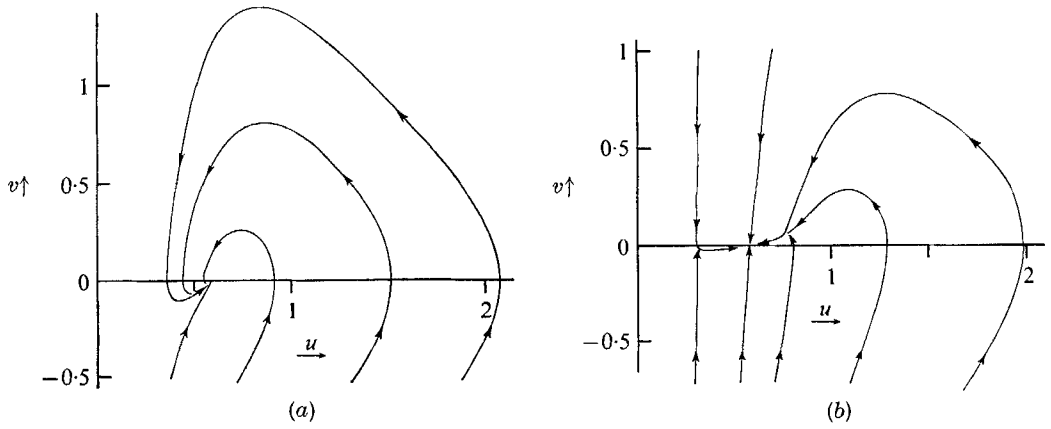

FIGURE 3. Phase plane for case 1, $T > 0$. Sketches of typical trajectories, arrows in the direction of x decreasing: (a) case 1(a), $(B/T^3)^{\frac{1}{2}} = \frac{1}{3}$; ($b$) case 1($c$), $(B/T^3)^{\frac{1}{2}} = \frac{5}{3}$. $v = s$, $u = r(B/T)^{\frac{1}{2}}$.

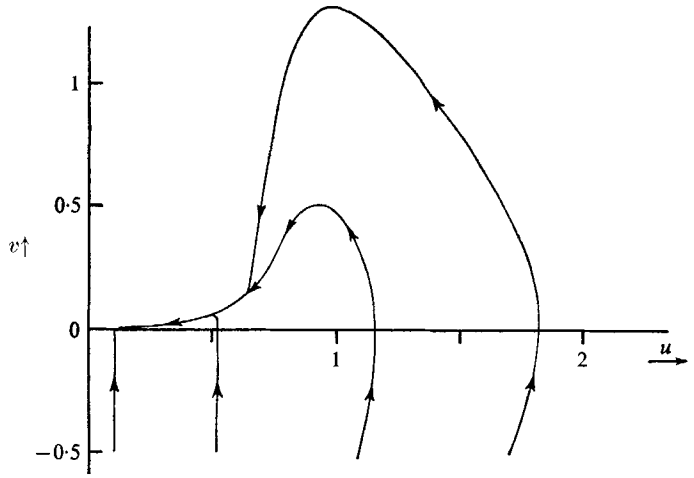

FIGURE 4. Phase plane for case 2, $T = 0$. Sketches of typical trajectories, arrows in the direction of x decreasing. $v = s$, $u = rB^{\frac{1}{3}}$.

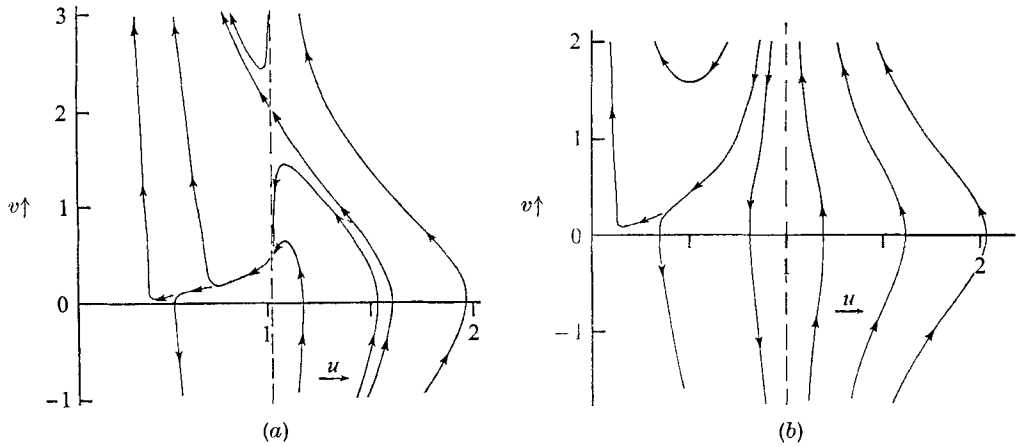

FIGURE 5. Phase plane for case 3, $T < 0$. Sketches of typical trajectories, arrows in the direction of x decreasing. (a) Case 3(a), $(-B/T^3)^{\frac{1}{2}} = \frac{5}{3}$; ($b$) case 3($c$), $(-B/T^3)^{\frac{1}{2}} = \frac{1}{3}$. $v = s$, $u = r(-B/T)^{\frac{1}{2}}$.

point, and $((T/3B)^{\frac{1}{2}}, 0)$, which is a focus in case 1(*a*) and a node in cases 1(*b*) and 1(*c*). This latter singular point is stable as ξ increases (x decreases, from the freeze-line towards the die). It can further be shown that there are no closed trajectories; hence, that every trajectory starting in $r > 0$ tends to $((T/3B)^{\frac{1}{2}}, 0)$ as $x \to -\infty$.

Case 2. The only singular point is the origin, which is a node, stable as ξ increases.

Case 3. The origin is a saddle-point; in case 3(*c*), this is the only singular point. In case 3(*b*), there is a saddle-node at $((-T/B)^{\frac{1}{2}}, 1)$. In case 3(*a*), the point $((-T/B)^{\frac{1}{2}}, q)$ is a node (stable as ξ increases); the point $((-T/B)^{\frac{1}{2}}, 1/q)$ is a saddle-point, where q is the smaller root of $4q^2 - 6(-B/T^3)^{\frac{1}{2}} q + 4 = 0$.

In case 3, $r < (-T/B)^{\frac{1}{2}}$ corresponds to $T + r^2 B < 0$; so in figure 5 the arrows on the trajectories (in the direction of x decreasing) show ξ decreasing for $r < (-T/B)^{\frac{1}{2}}$ and increasing for $r > (-T/B)^{\frac{1}{2}}$. For system (10), moreover, the points $((-T/B)^{\frac{1}{2}}, q)$ and $((-T/B)^{\frac{1}{2}}, 1/q)$ are not strictly speaking singular points, since they are not themselves solutions of the equations, and solutions tending to these points do in fact reach them in a finite distance (x). They are rather points of bifurcation of these solutions, where ds/dx ($= d^2r/dx^2$) is indeterminate. The physical interpretation of this non-uniqueness is discussed below. (See also appendix.)

3.2. *Results of the qualitative analysis*

First we discuss case 3, where T_Z is so small that there is a real, positive value of r, $r = (R^2 - T_Z/B)^{\frac{1}{2}}$, for which $T + r^2 B$ vanishes, and (7) becomes singular. From (6) (which is (4) in dimensionless form), we see that this means that the longitudinal tension in the bubble P_L vanishes at this value of r, so that the radius of curvature R_L in (5) is indeterminate. With this interpretation (that the film becomes slack), it is not surprising that our model fails to predict a unique shape for the bubble; to keep in touch with the practical process, we insist that the axial tension applied is sufficient to keep the film taut between the die and the freeze-line. It is sufficient for this to require that $T_Z > B(R^2 - 1)$.

Numerical solution of the equations (see below) shows that cases 2 and 3 give rise to large blow ratios R and very small freeze-line distances X and thickness reductions h_0/H compared with the values observed in practice, so subsequent discussion is based on case 1. As was mentioned above the qualitative analysis provides additional reasons for the choice of boundary condition that was made ($r' = 0$ at $x = X$). As x decreases (proceeding towards the die), the trajectories approach the singular point and, for large enough freeze-line heights, r' must be small at the die. (Computation suggests that r' will fall below 0·1, in a distance of about 3 die diameters, measured from the freeze-line.) Thus, the observed behaviour of the solutions is predicted without the necessity of imposing any condition at $x = 0$. A similar argument does not apply for x increasing, as we approach the freeze-line; moreover, d^2r/dx^2 is large far from the singular point, so that a small change in X would cause a large change in dr/dx at $x = X$ (i.e. the bubble shape would be critically dependent on X, and similarly on the other parameters, unless the condition on dr/dx is imposed at the freeze-line).

We can also make some numerical predictions for long bubbles, since all trajectories tend to the singular point $r = (T/3B)^{\frac{1}{2}}$, $r' = 0$, as $x \to -\infty$. Hence, as $X \to \infty$, the die radius tends to $(T/3B)^{\frac{1}{2}}$; since $r(0) = 1$, we have in the limit $T = 3B$, so that the blow ratio R tends to the value $(T_Z/B - 3)^{\frac{1}{2}}$. In case 1(*c*), provided R is not too large, r decreases monotonically from R to $(T/3B)^{\frac{1}{2}}$; so the die radius 1 must be greater than the latter value. Hence,

$$R^2 > T_Z/B - 3,$$

and we have a minimum blow ratio attained for large freeze-line distances. The numerical work confirms that this behaviour is relevant for values of the parameters in the practical range of interest; it also shows that the limiting value is nearly attained in many cases for freeze-line distances of about 10 times the die radius ($X \approx 10$).

Again, this limiting value is independent of liquid flow rate and viscosity, since $T_Z/B = F_Z/\pi a_0^2 \Delta$; it depends only on the applied forces and the die radius. For a long bubble, the blow ratio increases with increased axial tension, and with decreased die radius and internal pressure. This last result is less surprising when one recalls the behaviour of a spherical bubble acted on by an internal pressure and surface tension forces. (The excess pressure required to sustain the bubble is inversely proportional to its radius.)

We can use the foregoing to estimate the effect of increasing the freeze-line distance on the thickness reduction h_0/H. Once the bubble is long enough for the limiting value of R to be substantially attained, any increase in X corresponds to a lengthening of the neck of the bubble, where r is close to 1, and r' is close to 0. We consider freeze-line distances X_1 and X_2, with corresponding film thicknesses H_1 and H_2; if R is the same in both cases, we have

$$(h_0/H_1)/(h_0/H_2) = \exp \int_{X_2}^{X_1} \tfrac{1}{4}(1 + r'^2)\,(T + r^2 B)\,dx.$$

Between X_1 and X_2 (measuring from the freeze-line), $r \approx 1$ and $r' \approx 0$, so that

$$(h_0/H_1)/(h_0/H_2) \approx \exp\{B(X_1 - X_2)\}$$

(using $T/3B \approx 1$). Estimates obtained in this way are compared with computed values of the ratio H_2/H_1 in table 1.

Pressure difference (B)	0·1	0·1	0·1	0·2	0·2	0·3
Axial tension (T_Z)	0·5	0·5	2·0	1·0	2·5	2·0
Limiting blow ratio ($R = (T_Z/B - 3)^{\frac{1}{2}}$)	1·41	1·41	4·12	1·41	3·08	1·91
Lower freeze-line distance (X_2)	20	15	10	10	4	6
Upper freeze-line distance (X_1)	30	20	15	15	10	10
Estimate of H_2/H_1, $\exp(B(X_1 - X_2))$	2·72	1·65	1·65	2·72	3·32	3·32
Computed value of H_2/H_1	2·84	1·74	1·86	2·89	3·61	3·46

TABLE 1. Comparison of estimated and computed values of the change in thickness reduction due to a change in freeze-line distance

3.3. *Numerical results*

Numerical estimates of the bubble shape and thickness were obtained by a Runge–Kutta integration procedure, no special precautions being necessary. Values of B, T_Z, and X were fixed, R was guessed, and (7) was integrated from $x = X$ (with $r = R$ and $dr/dx = 0$) to $x = 0$. This process was repeated with improved guesses for R, until the condition $r = 1$ at $x = 0$ was satisfied.† Then (6) was integrated to give h_0/H (and $h_0/h(x)$ if desired). Some typical bubble shapes are shown in figure 6 for values of the parameters corresponding to cases 1 (*a*), 1 (*c*), 2 and 3 (*a*). The shape for case 1 (*c*) is similar to those observed in practice.

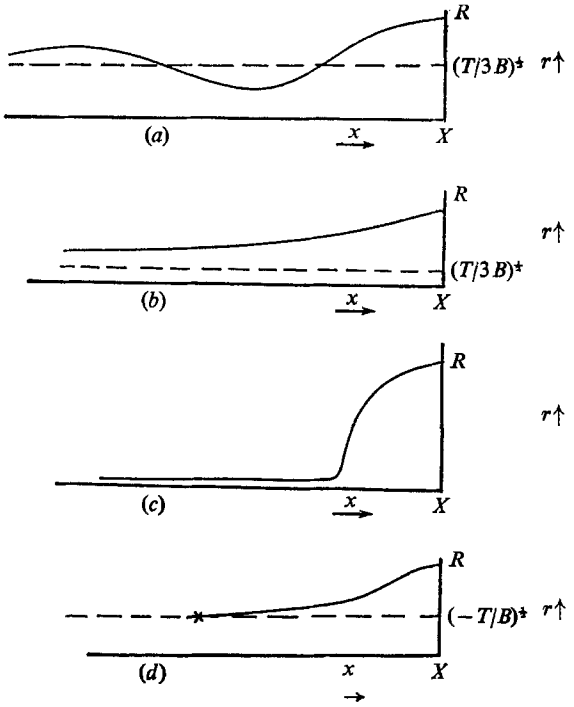

FIGURE 6. Sketches of typical bubble shapes: (*a*) case 1 (*a*), (*b*) case 1 (*c*), (*c*) case 2, (*d*) case 3 (*a*).

For the film-blowing process two of the important parameters are the product dimensions, which are determined by A and H, so the dimensionless ratios R ($= A/a_0$) and h_0/H are the quantities we wish to predict as functions of the dimensionless parameters B, T_Z and X (i.e. of the physical variables Δ, F_Z, Z, a_0, μ and Q). For results of practical interest, we may restrict attention to the ranges

† If no other information was available (e.g. from calculations with similar values of the parameters), R was chosen by linear interpolation. The first two values used in that case were $((T_Z/B) - 3)^{\frac{1}{2}}$, the limiting value of R as $X \to \infty$, and $(T_Z/B)^{\frac{1}{2}}$, the limiting value of R as the film tension was allowed to fall to zero at some point in a long film. In practice, the final value was often quite near the first of these values, as can be seen in figure 7.

$1{\cdot}5 \leqslant R \leqslant 3$, $10 \leqslant h_0/H \leqslant 30$ and $8 \leqslant X \leqslant 20$; hence, we have the restrictions $0{\cdot}075 \leqslant B \leqslant 0{\cdot}4$ and $0{\cdot}5 \leqslant T_Z \leqslant 2{\cdot}5$. It is not easy to estimate μ (since in practice it could vary from 10^4 to 10^6 poise along the film, on account of the variations of temperature, and, to a lesser extent, of shear rate); there are no data from which F_Z can be obtained (so far as we know). Thus, the above is probably the most reliable way of estimating the relevant values of the parameters. If we take the values (appropriate to a small-scale experimental arrangement) $a_0 = 3{\cdot}75$ cm, $Q = 4\,\mathrm{cm}^3/\mathrm{sec}$, $\Delta = 70\,\mathrm{N/m}^2$ ($\approx 7 \times 10^{-4}$ atmospheres), $\mu = 3 \times 10^5$ poise, and $F_Z = 5\,\mathrm{N}$ ($\approx 1\,\mathrm{lb.\ wt.}$), we obtain $B = 0{\cdot}097$ and $T_Z = 1{\cdot}56$.

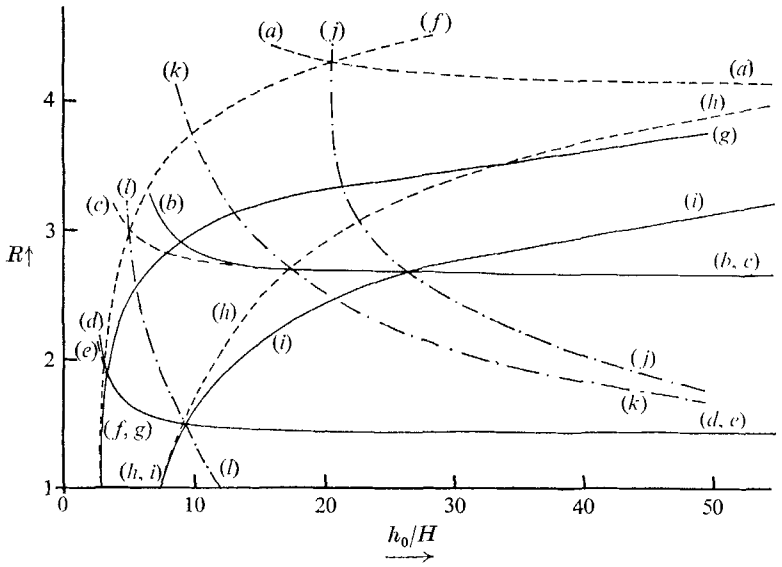

FIGURE 7. Typical results: Blow ratio R against thickness reduction h_0/H. Curves of constant B and T_Z, B and X, and T_Z and X. (*a*) $B = 0{\cdot}1$, $T_Z = 2$; (*b*) $B = 0{\cdot}2$, $T_Z = 2$; (*c*) $B = 0{\cdot}1$, $T_Z = 1$; (*d*) $B = 0{\cdot}2$, $T_Z = 1$; (*e*) $B = 0{\cdot}1$, $T_Z = 0{\cdot}5$; (*f*) $B = 0{\cdot}1$, $X = 10$; (*g*) $B = 0{\cdot}2$, $X = 5$; (*h*) $B = 0{\cdot}1$, $X = 20$; (*i*) $B = 0{\cdot}2$, $X = 10$; (*j*) $T_Z = 2$, $X = 10$; (*k*) $T_Z = 1$, $X = 20$; (*l*) $T_Z = 1$, $X = 10$.

Pressure difference (B)	0·2	0·175	0·165	0·1	0·09
Axial tension (T_Z)	2·3	2·0	1·85	1·15	1·0
Freeze-line distance (X)	8	9	10	20	23

TABLE 2. Typical values of the dimensionless parameters for blow ratio (R) = 3 and thickness reduction (h_0/H) = 20

The effect of the parameters B, T_Z and X on the product dimensions is shown in figure 7, where R is plotted against h_0/H for fixed values of pairs of these parameters. Table 2 shows how these parameters are interrelated by giving typical values of the three of them for $R = 3$ and $h_0/H = 20$. (One of B, T_Z and X can be chosen arbitrarily.)

As mentioned in § 1, the take-up of the film, which has here been assumed to imply a prescribed axial tension T_Z at the freeze-line, could be at constant velocity,

equivalent to fixing the axial velocity at the freeze-line. From continuity ($Q = 2\pi a h v_1$), we deduce that $R = v_1(0)\, h_0/v_1(X)\, H$, giving a straight line of slope $v_1(0)/v_1(X)$ on figure 7. Thus, fixing values of B and X (giving another line on figure 7), as well as this ratio, suffices to determine the solution of the problem. To compute a solution from these conditions, a value of T_Z would be guessed, and the value of T_Z needed to give the prescribed value of the ratio $v_1(0)/v_1(X)$ would be found by iteration.

3.4. *Neglected factors*

The effect on the feasibility of this approach to the analysis of the film-blowing process of some of the many neglected factors has been discussed from the point of view of the asymptotic analysis in part 1 (Pearson & Petrie 1970*a*). Here remarks will be confined to four topics where the less formal approach can be expected to be helpful. In particular, no mention is made here of gravity, inertia or effects due to a thick film. (In practice the ratio of film thickness to bubble radius will lie between 0·05 and 0·005 at the die, and will be smaller downstream.)

The details of the flow at the die exit, where the flow changes from a constrained to a free-surface flow, have been ignored, despite the quite large 'die-swell' effects observed in the flow of molten polymers. (See e.g. Pearson 1966, p. 48.) The assumption, that the effects of this transition are confined to a region near the die exit, allows the crude approach of 'correcting' the initial values a_0 and h_0 from the die dimensions to the values the die dimensions would have to take in the absence of any such effects, so as to give the same downstream flow. With the present state of knowledge of the transition flow, this is an empirical correction.

Air drag can perhaps be dealt with (iteratively if necessary), by taking the results of the above analysis in its absence, and calculating the air drag on a bubble of that fixed shape and velocity. Taylor (1959) leads one to hope that the effect will be small. (Taylor estimates a 7 % velocity reduction due to air drag on a water bell.)

The effect of surface tension can easily be allowed for in this approach, with the proviso that, if the surface tension forces are very much greater than the viscous forces, the film thickness is not found in the first approximation, since the equations replacing (6) and (7) become equivalent. We write $P_L + 2\Gamma$ and $P_H + 2\Gamma$ for P_L and P_H in (4) and (5), where Γ is the surface tension at the liquid–air interface, and then terms $\frac{1}{2}Gr\sec\theta$ and $2Gr^2\sec\theta$ are added to the right-hand sides of (6) and (7), respectively, where $G = 2\pi a_0^2\Gamma/\mu Q$, the ratio of surface tension to viscous forces. The modified equations have not been studied in detail, but the limiting value of R as $X \to \infty$ is readily obtained from

$$1 = \left(\frac{T}{3B}\right)^{\frac{1}{2}}\left\{\left[1+\frac{G^2}{3BT}\right]^{\frac{1}{2}}+\left[\frac{G^2}{3BT}\right]^{\frac{1}{2}}\right\}, \quad \text{where} \quad R^2 = (T_Z - T)/B,$$

and the phase plane is not altered in any major way for $T > 0$ and G not too large. The non-uniqueness in case 3 is not avoided by taking surface tension into consideration.

Temperature affects the mechanics of the flow through the dependence of viscosity on temperature; an attempt was made to estimate this effect by allowing μ to vary with position along the film. The viscosity was taken to be μ_0 at the

freeze-line, where it changes discontinuously as in all the models considered, and to decrease towards the die (with increasing temperature) in a predetermined way. Functions $\mu/\mu_0 = 1-0{\cdot}05(X-x)$, $\exp\{-0{\cdot}05(X-x)\}$ and $\exp\{-0{\cdot}5(X-x)\}$ were used for X up to 8, 8 and 10 respectively, giving viscosity reductions of 40 %, 33 % and 99 % over the length of the bubble. The bubble shape was not significantly altered in any of these cases, the major effect being a considerable increase in the thickness reduction h_0/H over the value it took in the constant viscosity case. This is in the main due to more rapid thinning of the film in the long neck of the bubble, where the liquid is hottest and least viscous. Obviously, this will have an important effect on the quantitative predictions, but it leaves the qualitative results substantially unaffected. A similar conclusion probably holds for the effect of the variation of viscosity with rate of shear.

4. Conclusions

We can, with reasonable confidence, deduce from the results of this work that the dominant factor controlling the flow is the balance between the viscous forces and the externally applied forces. The major shortcoming of the quantitative predictions (for the practical process of making thermoplastic film) is likely to arise from the neglect of the temperature variation and its effect on the liquid viscosity. The effects of surface tension and air drag are certainly worth investigating, but seem unlikely to affect the main features of the flow. In large bubbles of thick film being slowly drawn, gravity becomes a limiting factor.

Part of the work reported here was carried out while one of us (C. J. S. P.) held a Science Research Council Fellowship in the Department of Chemical Engineering at Cambridge. We are grateful to the Science Research Council, and to the Head of the Department, for enabling us to carry out this work. Some of the computational work was done in the computing laboratories of Cambridge and of Newcastle upon Tyne Universities; we are also grateful to the directors of these laboratories for the use of their facilities.

Appendix. The phase plane for system (11)

$$\left.\begin{aligned} dr/d\xi &= -2r^2s(T+r^2B), \\ ds/d\xi &= -6s-r(1+s^2)(T-3r^2B). \end{aligned}\right\} \tag{11}$$

(i) The origin is a non-elementary singular point to which the theorems of Keil (Sansone & Conti 1964, pp. 256–267) may be applied. For $T \neq 0$ (cases 1 and 3), we write $u = Tr$, $v = 6s+Tr$, $t = 6\xi$, and $A = B/T^3$, to obtain

$$\left.\begin{aligned} du/dt &= g(u,v), \\ dv/dt &= v+f(u,v), \end{aligned}\right\} \tag{A 1}$$

where $$f(u,v) = \tfrac{1}{36}u(v^2-u^2(1+108A))-\tfrac{1}{36}Au^3(v-u)(3v-5u),$$

and $$g(u,v) = \tfrac{1}{18}u^2(v-u)(1+Au^2).$$

We identify (v, u) with (x, y) of Keil's theorems, and see that system (A 1) satisfies the hypotheses of the theorems; namely, that f and g are dominated by linear terms near $(0, 0)$, and that in a neighbourhood of $(0, 0)$, excluding $(0, 0)$ itself, du/dt and dv/dt do not both vanish.

From the first theorem, there are two and only two trajectories tangent to the v-axis at the origin, and for system (A 1) these are clearly the half-lines $u = 0$, $v > 0$ and $u = 0$, $v < 0$. The two regions, into which this pair of trajectories divides the plane, are considered separately; from the second theorem, the trajectories in each region fall into one of two classes: either (1) all trajectories are parabolic (i.e. they tend to the origin) and tangent to the u-axis at the origin, or (2) one trajectory is parabolic and tangent to the u-axis at the origin, while all the other trajectories are hyperbolic (as are the trajectories near a saddle-point). Thus, the origin is either a node ((1) in both regions), a saddle-point ((2) in both regions), or a saddle-node ((1) in one region and (2) in the other region).

We distinguish between these alternatives by means of the third theorem, by studying the slope dv/du of trajectories on either side of the isocline J_0 (where $dv/du = 0$). We consider first the half-plane $u > 0$, where, if dv/du increases with v increasing across J_0, we have (1), and, if dv/du decreases, we have (2). The converse is true in the half-plane $u < 0$.

Here we approximate J_0 near the origin by

$$v = \tfrac{1}{36}(1 + 108A)\,u^3 + \tfrac{5}{36}Au^5,$$

so that for $A > -1/108$ J_0 lies in the first and third quadrants ($uv > 0$). On $v = 0$, dv/du is given by

$$dv/du = (-u^3(1 + 108A) - 5Au^5)/\{-2u^3(1 + Au^2)\},$$

which is positive near the origin for $A > -1/108$, so that, from continuity arguments, dv/du in this case decreases as J_0 is crossed in the direction of v increasing. (And, in $u < 0$, it increases.) For $A \leqslant -1/108$, J_0 lies in the second and fourth quadrants, and dv/du is negative near the origin, leading to the same conclusion. Thus, for all values of A, the origin is a saddle-point with separatrices tangent to the u- and v-axes (i.e. the separatrices are the lines $r = 0$ and $6s + Tr = 0$ in the (r, s)-plane). (See figures 3 and 5.)

For $T = 0$, we set $u = rB^{\frac{1}{4}}$, $v = s$ and $t = -6\xi$ to obtain

$$\left.\begin{aligned} du/dt &= \tfrac{1}{3}u^4v, \\ dv/dt &= v - \tfrac{1}{2}u^3(1 + v^2), \end{aligned}\right\} \tag{A 2}$$

and apply the same methods. (See figure 4.)

(ii) At the singular point $((T/3B)^{\frac{1}{2}}, 0)$ of case 1 the equations are, writing $w = r - (T/3B)^{\frac{1}{2}}$,

$$dw/d\xi = (8T^2/9B)\,s + O(w^2 + s^2),$$

$$ds/d\xi = -2Tw + 6s + O(w^2 + s^2).$$

The standard methods (see e.g. Sansone & Conti 1964, pp. 44–47) lead to the results that the point $((T/3B)^{\frac{1}{2}}, 0)$ is a stable focus for $16T^3/9B > 9$, and a stable node for $16T^3/9B \leqslant 9$. In the latter case, the critical directions are given by $s/w = \frac{27}{8}(B/T^3)^{\frac{1}{2}}[1 \pm (1 - 16T^3/81B)^{\frac{1}{2}}]$.

(iii) Similarly, the results stated in the main text for the singular points of case 3(*a*) can be obtained from

$$d(r-(-T/B)^{\frac{1}{2}})/d\xi = -4q(-T^3/B)^{\frac{1}{2}}(r-(-T/B)^{\frac{1}{2}}) + O((r-(-T/B)^{\frac{1}{2}})^2+(s-q)^2),$$
$$d(s-q)/d\xi = -10(q^2+1)T(r-(-T/B)^{\frac{1}{2}}) + (8q(-T^3/B)^{\frac{1}{2}}-6)(s-q) + O((r-(-T/B)^{\frac{1}{2}})^2+(s-q)^2),$$

for the point $(1, q)$, and

$$d(r-(-T/B)^{\frac{1}{2}})/d\xi = -(4/q)(-T^3/B)^{\frac{1}{2}}(r-(-T/B)^{\frac{1}{2}}) + O((r-(-T/B)^{\frac{1}{2}})^2+(s-1/q)^2),$$
$$d(s-1/q)/d\xi = -(10T(q^2+1)/q^2)(r-(-T/B)^{\frac{1}{2}}) + (8(-T^3/B)^{\frac{1}{2}}/q-6)(s-1/q) + O((r-(-T/B)^{\frac{1}{2}})^2+(s-1/q)^2)$$

where $q = \frac{3}{4}(-B/T^3)^{\frac{1}{2}} - ((-9B/16T^3)-1)^{\frac{1}{2}}$, and $0 > T^3 > -9B/16$.

(iv) In case 3(*b*), we write $u = r-(-T/B)^{\frac{1}{2}}$, $v = s-1$ to obtain

$$du/d\xi = -3u + O(u^2+v^2),$$
$$dv/d\xi = 15(-B/T)^{\frac{1}{2}}u + O(u^2+v^2),$$

so that $u = v = 0$ is a non-elementary singular point, which may be shown to be a saddle-node. (Sansone & Conti 1964, pp. 256–267.)

(v) In case 3, solutions with dr/dx tending to ∞ are possible and we can get more information by considering the (r, θ)-plane, where $\tan\theta = dr/dx$; i.e. we have as phase space the surface of a cylinder rather than a plane. System (11) becomes

$$\left.\begin{aligned} du/dt &= -2u^2(u^2-1)\sin\theta, \\ d\theta/dt &= \cos\theta(u(1+3u^2) - m\sin 2\theta), \end{aligned}\right\} \tag{A 3}$$

where $u = r(-B/T)^{\frac{1}{2}}, \quad m = 6(-B/T^3)^{\frac{1}{2}}$

and $dt/dx = -(-T^3/B)^{\frac{1}{2}}/2r^2(T+r^2B)\cos\theta.$

In case 3(*a*), system (A 3) has six singularities on $u = 1$ and a further four on $u = 0$ in $-\pi < \theta \leqslant \pi$. Writing α for the smallest positive root of

$$\sin 2\theta = 4/m \quad (0 < \alpha < \tfrac{1}{4}\pi),$$

these are $(1, \alpha)$, $(1, \frac{1}{2}\pi-\alpha)$, $(1, \frac{1}{2}\pi)$, $(1, -\pi+\alpha)$, $(1, -\frac{1}{2}\pi-\alpha)$, $(1, -\frac{1}{2}\pi)$ and $(0, 0)$, $(0, \frac{1}{2}\pi)$, $(0, \pi)$, $(0, -\frac{1}{2}\pi)$. Solutions relevant to the physical problem start on $\theta = 0$ with $u > 1$ (at the freeze-line) and such solutions, and in fact any solutions starting in $u > 1$, reach either the singularity $(1, \alpha)$ or $(1, \frac{1}{2}\pi)$, apart from the separatrices approaching $(1, \frac{1}{2}\pi-\alpha)$ and leaving $(1, -\frac{1}{2}\pi)$. At these singularities, the solution of system (10) is indeterminate, but there are only certain possibilities open to it. For example, solutions leaving $(1, \alpha)$, apart from the ingoing separatrix to the origin, must approach either $(1, -\frac{1}{2}\pi)$ or $(0, \frac{1}{2}\pi)$, and, by such arguments, certain types of solution can be predicted. The investigation of the solutions of the equations in this case are not discussed in more detail here, because they are not relevant to the particular physical problem motivating the analysis.

(vi) The proof that in case 1 all trajectories in $r > 0$ tend to the singular point $((T/3B)^{\frac{1}{2}}, 0)$ depends on showing that there is a family of closed curves in this half-

plane, which are always crossed from their exterior to their interior by trajectories as x decreases. System (11) may be written

$$\frac{dv}{du} = \frac{mv + u(1-3u^2)(1+v^2)}{2u^2(1+u^2)v}$$

(where $u = r(T/B)^{\frac{1}{2}}$, $t = \xi(T^3/B)^{\frac{1}{2}}$, $m = 6(B/T^3)^{\frac{1}{2}}$ and $v = s$), which can be integrated to give

$$v^2 = Au/(1+u^2)^2 - 1 + E(u),$$

where $A = (1+U)^2(1+V^2)/U$ for the trajectory passing through the point (U, V), and

$$E(u) = \frac{u}{(1+u^2)^2}\int_U^u mv\frac{(1+y^2)}{y^3}dy.$$

Writing $v_1^2 = Au/(1+u^2)^2 - 1$, we see that the curves $v^2 = v_1^2$ are closed, symmetrical about $v = 0$, and cut $v = 0$ once between $u = 0$ and $u = 1/\sqrt{3}$, and once for $u > 1/\sqrt{3}$. (A as defined above is never less than $\frac{16}{9}\sqrt{3}$, that minimum value giving a real value (0) for v only at $u = 1/\sqrt{3}$.)

We treat v_1 as an approximation to v with error E, and show that E is always such that $|v| < |v_1|$ as we proceed in the direction of x decreasing. Now $m > 0$, $u > 0$, and for $v > 0$ u decreases with x decreasing along a trajectory, so we take $u < U$, and see immediately that $E < 0$. Similarly, for $v < 0$, we take $u > U$, and again $E < 0$, so that $v^2 < v_1^2$, which is the desired result. Since the family of curves $v^2 = v_1^2$ fills the half-plane $u > 0$, this completes the proof.

REFERENCES

Novozhilov, V. V. 1959 *The Theory of Thin Shells.* Groningen: Noordhoff.

Pearson, J. R. A. 1966 *Mechanical Principles of Polymer Melt Processing.* Oxford: Pergamon.

Pearson, J. R. A. & Petrie, C. J. S. 1970*a* *J. Fluid Mech.* **40**, 1.

Pearson, J. R. A. & Petrie, C. J. S. 1970*b* *Plastics & Polymers*, **38**, 85.

Sansone, G. & Conti, R. 1964 *Non-linear Differential Equations.* Oxford: Pergamon.

Taylor, G. I. 1959 *Proc. Roy. Soc.* A **253**, 289–295.